Accepted Manuscript

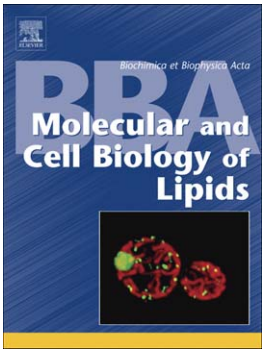

Nanotubes connecting B lymphocytes: High impact of differentiation-dependent lipid composition on their growth and mechanics

Eszter A. Tóth, Ádám Oszvald, Mária Péter, Gábor Balogh, Anikó Osteikoetxea-Molnár, Tamás Bozó, Edina Szabó-Meleg, Miklós Nyitrai, Imre Derényi, Miklós Kellermayer, Toshiyuki Yamaji, Kentaro Hanada, László Vígh, János Matkó

PII: S1388-1981(17)30115-4
DOI: doi:10.1016/j.bbalip.2017.06.011
Reference: BBAMCB 58167

To appear in: *BBA - Molecular and Cell Biology of Lipids*

Received date: 31 January 2017
Revised date: 16 May 2017
Accepted date: 17 June 2017

Please cite this article as: Eszter A. Tóth, Ádám Oszvald, Mária Péter, Gábor Balogh, Anikó Osteikoetxea-Molnár, Tamás Bozó, Edina Szabó-Meleg, Miklós Nyitrai, Imre Derényi, Miklós Kellermayer, Toshiyuki Yamaji, Kentaro Hanada, László Vígh, János Matkó, Nanotubes connecting B lymphocytes: High impact of differentiation-dependent lipid composition on their growth and mechanics, *BBA - Molecular and Cell Biology of Lipids* (2017), doi:10.1016/j.bbalip.2017.06.011

BBA Molecular and Cellular Biology of Lipids

Original research article

Nanotubes connecting B lymphocytes: High impact of differentiation-dependent lipid composition on their growth and mechanics

Eszter A. Tóth[1], Ádám Oszvald[1], Mária Péter[2], Gábor Balogh*[,2], Anikó Osteikoetxea-Molnár[1], Tamás Bozó[3], Edina Szabó-Meleg[4,5], Miklós Nyitrai[4,5], Imre Derényi[6], Miklós Kellermayer[3,7], Toshiyuki Yamaji[8], Kentaro Hanada[8], László Vígh[2], János Matkó[*,1]

[1]Department of Immunology, Eötvös Lorand University, Budapest, Hungary;
[2]Institute of Biochemistry, Biological Research Centre of the Hungarian Academy of Sciences, Szeged, Hungary;
[3]Department of Biophysics and Radiation Biology, Semmelweis University, Budapest, Hungary;
[4]Department of Biophysics, Medical Faculty, University of Pécs, Pécs, Hungary Department of
[5]Szentágothai Research Center, University of Pécs, Pécs, Hungary;
[6]Department of Biological Physics, Eötvös Lorand University, Budapest, Hungary;
[7]MTA-SE Molecular Biophysics Research Group, Semmelweis University, Budapest, Hungary;
[8]Department of Biochemistry and Cell Biology, National Institute of Infectious Diseases, Shunjuku-ku, Tokyo, Japan.

[*]**Correspondence**: János Matkó, Eötvös Lorand University, Department of Immunology (e-mail: janos.matko@ttk.elte.hu) and Gábor Balogh, Institute of Biochemistry, Biological Research Centre of the Hungarian Academy of Sciences, Szeged, Hungary (e-mail: balogh.gabor@brc.mta.hu)

Keywords: B cell membrane nanotubes; lipidomics; cholesterol; sphingolipids; lipid order/fluidity; membrane mechanics;

Short title: Lipid-control on B lymphocyte nanotubular connections

Highlights:

- Nanotubular connections of B cells depend on their maturation/differentiation
- NT-growing capacity correlates with membrane lipid composition
- Outer and inner layer lipids facilitating membrane curvature promote NT growth
- Targeted depletion of raftophilic lipids suppresses NT formation between B cells
- Membrane lipid order modulates growth of the highly stable, elastic B cell NTs

List of abbreviations: PM: plasma membrane; NT: nanotube; CTX-B: cholera toxin B subunit; PUFA: polyunsaturated fatty acid; Cer, ceramide; GlcCer, glucosyl ceramide; LacCer, lactosyl ceramide; GM3, monosialodihexosylganglioside; DHA: docosahexaenoic acid; CERT: ceramide transporter; ECM: extracellular matrix; LA: linoleic acid; PI(4,5)P2: phosphatidylinositol-(4,5)-bis-phosphate; LC-CLSM: live cell confocal laser scanning microscopy; MBCD: methyl-β-cyclodextrin; AFM: atomic force microscopy; GSL: glycosphingolipid; SM: sphingomyelin.

Abstract

Nanotubes (NTs) are thin, long membranous structures forming novel, yet poorly known communication pathways between various cell types. Key mechanisms controlling their growth still remained poorly understood. Since NT-forming capacity of immature and mature B cells was found largely different, we investigated how lipid composition and molecular order of the membrane affect NT-formation. Screening B cell lines with various differentiation stages revealed that NT-growth linearly correlates with membrane ganglioside levels, while it shows maximum as a function of cholesterol level. NT-growth of B lymphocytes is promoted by raftophilic phosphatidylcholine and sphingomyelin species, various glycosphingolipids, and docosahexaenoic acid-containing inner leaflet lipids, through supporting membrane curvature, as demonstrated by comparative lipidomic analysis of mature versus immature B cell membranes. Targeted modification of membrane cholesterol and sphingolipid levels altered NT-forming capacity confirming these findings, and also highlighted that the actual lipid raft number may control NT-growth via defining the number of membrane-F-actin coupling sites. Atomic force microscopic mechano-manipulation experiments further proved that mechanical properties (elasticity or bending stiffness) of B cell NTs also depend on the actual membrane lipid composition. Data presented here highlight importance of the lipid side in controlling intercellular, nanotubular, regulatory communications in the immune system.

1. Introduction

Intercellular communication between cells of the innate and adaptive immune systems has emerged as essential to regulatory pathways that control both cellular and humoral immune responses. Such pathways are mediated by secreted cytokines [1] or by secretion and subsequent reuptake of membrane microvesicles [2,3] over large distances without direct intercellular contact. An alternative mode of intercellular communication is formation of immunological synapses based on cell-cell contacts [4,5]. Long-distance (up to 200 μm) nanotubular connections [6–9] have also been reported as novel communication pathways. Membrane nanotubes (NTs; whereas open-ended versions are often called tunneling nanotubes) are rich in actin filaments and sometimes also in microtubules which comprise the molecular skeleton for these nanostructures [8]. NTs may provide routes for extensive exchange of information (specific signals) or biomatter between cells. Trafficking of vesicles [10], calcium ions [11], viral proteins [12], bacteria [10], cytoplasmic molecules, organelles, plasma membrane (PM) components or mRNA [9,11] were observed either inside NTs or on their outer surfaces, suggesting involvement of various motor proteins (myosins, dyneins, or kinesins). Such processes can influence cell development, differentiation, effector functions or cell death in both the innate and adaptive immune systems [13]. However, the particular role of NTs in immunoregulation, especially in pathological situations, still remained poorly explored.

Despite the continuously accumulating knowledge about NTs, little is known about the external and cellular factors or mechanisms that control their growth initiation or regulate their lifetime and retraction. NTs can grow between daughter cells following cell division or separation of cells after resolution of immunological synapse [14]. Little is known, however, about how the lipid composition of the plasma membrane controls NT growth and mechanical properties in live cells. Cholesterol and other raft lipids have a significant impact on signal

transduction across the PM and on subsequent cellular responses of lymphocytes. Depletion of membrane cholesterol was shown to influence the lateral mobility of membrane proteins depending on whether they are cytoskeleton-associated or not and, thus, has a global effect on cell and PM architecture [15]. Differentiation/maturation and tumorous transformation are usually accompanied with substantial changes in lipid composition and microstructure of the PM [16–18]. These facts may also be implicated in the NT forming capability of lymphocytes.

Here we first examined if membrane lipid composition can affect the frequency of NT formation at all. B lymphocytes, key cellular components of the humoral immune response, were selected for these investigations because their NT connections have not yet been studied in detail, in contrast to other immune cells [7,8]. This study was also initiated by the observation that immature B cells, in contrast to mature ones, could not grow NTs under the same conditions [19]. Thus, nine murine and human B cell lines representing various maturation or differentiation stages were investigated for NT formation capacity with statistical imaging in correlation with analysis of the membrane lipid composition by lipidomic analysis. It was anticipated that such a screening would help to identify key lipid species controlling NT growth or retraction.

How selective, targeted modifications of raft lipid levels or membrane plasticity (modulated through changing lipid ordering) can affect NT formation of B cells was also studied. Since dynamic tension and molecular order of PM may also be critical factors in NT growth, the effect of PM hyperfluidization by polyunsaturated fatty acid (PUFA) treatment on NT formation capacity was also investigated. B cells and the connecting NTs were characterized in terms of membrane lipid packing density by imaging di-4-ANEPPHQ polarimetric probe fluorescence and analyzing the generalized polarization [20,21]. Finally, we also examined the mechanical stability of NTs and their sensitivity to environmental mechanical effects/stress. These properties, including the effects of lipid modifications on the

mechanical properties of NTs, were probed by atomic force microscopy (AFM) mechano-manipulation experiments.

Our results suggest that the actual PM level of some inverted cone-shaped membrane lipids and known raft constituents, such as cholesterol, sphingomyelin (SM), glycosphingolipids (GSLs), are key lipid determinants promoting NT formation by mediating membrane curvature. Alternatively, as organized membrane microdomains, lipid rafts may provide a stable coupling between the membrane bilayer and the lymphocyte cortical cytoskeleton during formation or retraction of NTs. PUFAs may also regulate NT growth by assuring optimal membrane fluidity for the process. The data presented here for B lymphocytes may aid in understanding how the formation and mechanical stability/plasticity of NTs interconnecting immune cells are controlled at the cellular lipid level and also highlights that these properties strongly depend on the maturation/differentiation stage of a particular cell lineage.

2. Materials and methods

2.1. Cell culture

A20 (ATCC TIB208) and 2PK3 (ATCC TIB-203) mature murine B lymphoma, X16C murine transitional marginal zone B cell (ATCC TIB-209), 1-305 pre-B cell line, 38C13 immature murine B cell line [22,23], BL41 (DSMZ MUTZ: ACC 160), Daudi (ATCC CCL-213), BJAB (DSMZ: ACC 757) human Burkitt lymphoma cell lines and JY B lymphoblast cell line [24] were cultured in RPMI-1640 (Sigma-Aldrich) medium. All HeLa mutants [25] were cultured in Dulbecco's modified Eagle's medium (Sigma-Aldrich). The media were all supplemented with L-glutamine, Na-pyruvate, 2-mercaptoethanol, $NaHCO_3$, penicillin, streptomycin-sulfate, non-essential amino acids, vitamins and 10% FCS. Cells were cultured and treated at 37 °C in a 5% CO_2 incubator unless specified otherwise.

2.2. Cell treatments, membrane modifications

A20 cells were cultured in growth medium complemented with 2-50 µM Simvastatin (Sigma-Aldrich) (inhibitor of HMG-Coenzyme A reductase) for 24 h. To deplete membrane cholesterol or inhibit sphingolipid biosynthesis, A20 cells were treated with 0.5-10 mM methyl-beta-cyclodextrin (MBCD; CycloLab Ltd. Budapest) or with 1.5-14 µM Fumonisin B1 (Santa Cruz) in Hank's buffer (pH 7.4) for 15 min or 24 h, respectively. Cells were then washed and analysed by AFM or labeled with 1,1'-dioctadecyl-3,3,3'3'-tetramethylindocarbocyanine perchlorate (DiI, Invitrogen) for live cell confocal laser scanning microscopic (LC-CLSM) analysis of NT growth. In order to fluidize B cell membranes, linoleic acid (LA; 110-430 µM) (Sigma-Aldrich) or docosahexaenoic acid (DHA; 5-20 µM) (Sigma-Aldrich) were used for 30 min. After washing, cells were analysed by AFM or labeled with DiI for analysis of NT growth. For crosslinking of gangliosides, A20 cells were labeled with 40 µg/ml Alexa-488-conjugated CTX-B (Life Technologies) for 15 min at 4 °C. After washing, 100 µg/ml anti-choleratoxin antibody was added in serum-free

medium, then following a 20-min incubation in a CO_2 incubator, 10% FCS was added to complete the medium for NT growth.

2.3. Lipidomic analysis

Lipid standards were obtained from Avanti Polar Lipids. The solvents used for extraction and for mass spectrometric analyses were of liquid chromatographic grade from Merck and Optima LCMS grade from Thermo Fisher Scientific. All other chemicals were purchased from Sigma-Aldrich and were of the best available grade.

After treatment, cells were centrifuged in Eppendorf tubes (10^7 cells per tube), and the pellets were shaken in 1 mL methanol (containing 0.001% butylated hydroxytoluene as antioxidant) for 10 min, and centrifuged at 10000 x *g* for 5 min. The supernatant was transferred into a new Eppendorf tube and stored at −20 °C.

Mass spectrometric analyses were performed on a LTQ-Orbitrap Elite instrument (Thermo Fisher Scientific) equipped with a robotic nanoflow ion source TriVersa NanoMate (Advion BioSciences) with slight modifications relative to described previously [26]. Lipid classes and species were annotated according to the classification systems for lipids [27] and lipids were identified by LipidXplorer software [28]. Further details of measurements are presented in the Supplementary Materials and methods. Lipidomic results are presented as mean ±SEM; significance was determined according to Storey and Tibshirani [29] and was accepted at $p<0.05$ corresponding to a false discovery rate <0.015.

2.4.Flow cytometry

Ganglioside and cholesterol levels of PM were measured by BD FACS Aria III flow cytometer (Becton Dickinson). Cells were labeled with 40 µg/ml Alexa-488-conjugated cholera toxin B subunit (Life Technologies) for 20 min at 4 °C for ganglioside expression or with 100 µg/ml AC8 cholesterol-specific IgG3 antibody [30,31] for 45 min on ice for

cholesterol expression. AC8-Ab was then detected with Alexa488-GAMIG secondary antibody.

2.5. Microscopic analysis of NT growth

To statistically analyze NT growth, 10 µg/ml fibronectin (Sigma Aldrich, RT, overnight; or alternatively 10 µg/ml laminin) coats were used on borosilicate chamber microplate wells (Ibidi Planegg/Martinsried). After 1 h incubation, live cell snapshot images were taken at closely physiological conditions (37±0.1°C; CO_2:5%), at $3x10^5$ cells/well density. For visualizing NT growth, cells were labeled with 5 µM DiI dye (Life Technologies) for 5 min at 37 °C. DIC and fluorescence images of cells were recorded with Fluoview500/IX-81 inverted Laser Scanning Confocal Microscope (Olympus), using a 60x oil immersion objective (N.A.:1.1). High resolution static NT images were also recorded by scanning electron microscopy (ZEISS EVO 40XVP) of cells incubated on fibronectin coat for 2 hours, then fixed and dehydrated. NT formation statistics were calculated from at least 800 cells/sample and reported as mean ± SD or ±SEM as indicated. The frequency of NT-forming cells was defined as the ratio of cells growing at least one NT to the total cell number in the given field. The analysis was made using ImageJ software (Wayne Rasband, NIH; using plugins available at website: Wright Cell Imaging Facility, Toronto, ON, Canada) and the significance was analyzed using the Student's unpaired t-test in GraphPad Prism v5.0 statistics software.

2.6. Image analysis of lipid ordering

Di-4-ANEPPDHQ (Life Technologies) polarimetric fluorescent probe was used to detect lipid order in the B cell membranes or NTs, using a method described previously [21]. After labeling, cellular fluorescence intensity was recorded with Fluoview500 confocal microscope (Olympus) using 60x oil immersion objective (N.A.:1.1) in two emission channels ($\Delta\lambda_1$: 505-560 nm and $\Delta\lambda_2$: >610 nm) using excitation with the 488 nm line of an Ar ion laser. The analysis was performed using ImageJ software. Generalized polarization (GP)

values, providing information about membrane lipid packing density, were derived as follows:

$$GP=(I_{505\text{-}560})\text{-}(GxI_{>610})/(I_{505\text{-}560})+(GxI_{>610}),$$

where I values are the pixel fluorescence intensities recorded at the indicated spectral channel and G is a correction factor. GP can range from -1 (fully fluid, least packed membrane) to +1 (ideally tightly packed, ordered membrane) [21].

2.7. Atomic Force Microscopy and Spectroscopy (AFM)

AFM images were collected with an MFP3D instrument (Asylum Research) from cells (untreated or treated) incubated on fibronectin coat for 2 h. NTs were mechanically manipulated with an MFP3D AFM system mounted on an Olympus IX81 inverted microscope operating both in phase contrast and total internal reflection fluorescence modes [32]. Nanomanipulation was carried out with a silicon nitride cantilever (MSCT-AUHW, Veeco; D lever, nominal resonance frequency and spring constant 15 kHz and 0.03 N/m, respectively). The cantilever tip was calibrated by using the thermal method [33] yielding a typical spring constant of 0.03-0.04 N/m. Phase contrast video recordings were collected about the manipulated NTs at 25 frames/s with a color CCD camera (CP410 Panasonic). For further details see Supplementary Materials and methods.

3. Results

3.1. Nanotube growth between B cells depends on their maturation/differentiation-dependent membrane lipid composition

Microscopic images (Figure 1) demonstrate presence of interconnecting NTs in mature mouse (Figure 1A and E) and in human Daudi (Figure 1B) B cell lines. No NT formation and a rounded cell morphology were observed under the same conditions and cell densities in

murine immature or pre-B cell cultures (Figure 1C and also Figure 2 B,C,E,F) or in transformed Burkitt lymphoma cells (Figure 1D).

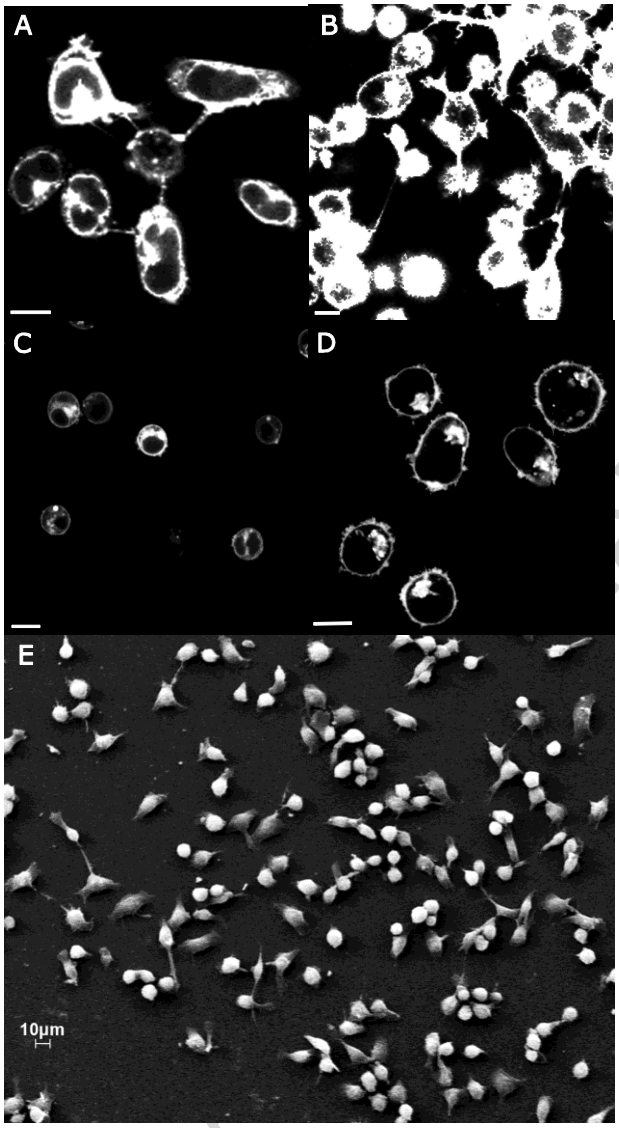

Figure 1. B cells form nanotubular connections depending on their maturation/ differentiation. Mature mouse A20 (**A**) and human Daudi B cells (**B**) spontaneously form nanotubular networks under near-physiological conditions (37°C, 5% CO_2 and fibronectin coat), as shown in representative LC-CLSM images. Cells were stained with DiI cell tracker dye. In contrast, 38C13 immature murine B cells (**C**) or BL41 human Burkitt lymphoma cells (**D**) did not show cell spreading or NT formation under the same conditions (scale bar: 10 µm). A representative scanning electron micrograph of A20 B cell nanotubular network on a fibronectin coat (**E**) is also shown. 1 column width

Therefore, the nine different B cell lines were characterized for the correlation between their PM ganglioside and cholesterol expression levels (probed by fluorescent cholera toxin B and AC8 monoclonal IgG3 antibody [30,31], respectively) and their NT-forming capacity. CTX-B-binding level linearly correlated with NT-frequency in all cells (Figure 2A-F), except 1-305 pre-B cells. Membrane staining of NTs showed a patchy ganglioside labeling (Figure 2G), indicating presence of lipid raft microdomains along the NTs. The high linear correlation (R^2=0.87) between ganglioside expression and NT-frequency (Figure 2H) points to an essential role of gangliosides in NT formation. In contrast, membrane cholesterol level exhibited a weak linear correlation (R^2=0.16) with NT-frequency in the same B cells, but instead represented a Gaussian relationship (R^2=0.80; Figure 2I), suggesting that NT growth requires an optimal membrane cholesterol level.

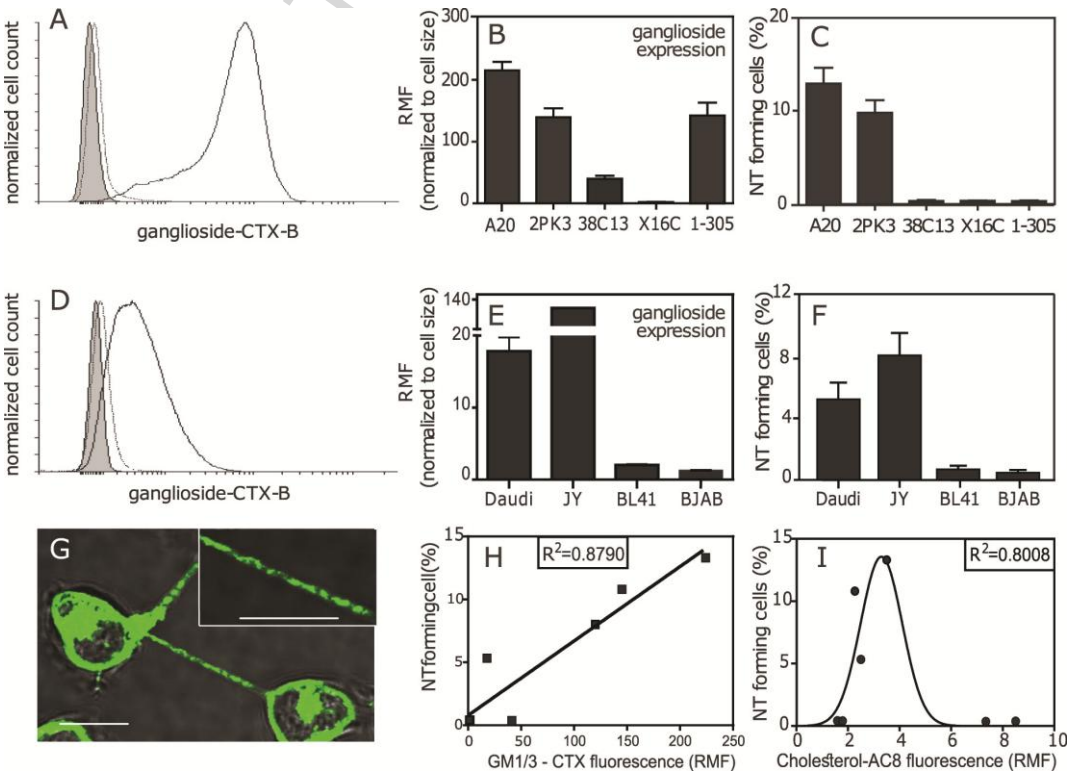

Figure 2. Correlation between NT formation frequency and membrane levels of gangliosides and cholesterol in B cell lines representing various differentiation/

maturation stages. (Murine B cells: A20, 2PK3: mature; 38C13: immature; X16C: transitional marginal zone; 1-305: pre-B cell phenotype; Human B cells: Daudi: mature B lymphoma cell, JY: EBV-transformed B lymphoblast, BL41 and BJAB are of Burkitt lymphoma phenotype). Representative flow cytometric histograms for ganglioside staining with Alexa488-choleratoxin-B (CTX-B) are shown for mature A20 (solid line) and immature 38C13 (dotted line) murine B cells (autofluorescence shown as light grey) (**A)**, as well as for human Daudi (solid line) and BL41 (dotted line) B cells (autofluorescence shown as light grey) **(D**), respectively. Results of at least three independent experiments of ganglioside expression and NT formation frequency (mean ± SEM) measurements for each cell line are also displayed (**B, C, E, F)**. Relative Mean Fluorescence (RMF) is the ratio of mean fluorescence and mean autofluorescence for the flow cytometric histograms shown (in panels A and D). NTs show typical patchy ganglioside staining (**G**) indicating existence of lipid raft microdomains along NTs (see also enlarged insert). Correlations between the membrane ganglioside level (**H**), as well as membrane cholesterol level (**I**), and the NT formation frequency are shown. The correlation was characterized by linear regression analysis or fitting to the Gaussian distribution function, respectively (R^2 correlation coefficient values are shown). (Scale bar: 10 μm)

2-column width

Since immature and mature B cells showed remarkable difference in NT-forming capacity, next we characterized two B cell lines representing strongly NT-forming and non-forming cells (mature A20 and immature 38C13 cells, respectively) in detail by high-sensitivity, high-resolution shotgun mass spectrometric lipidomic analysis. Altogether ~275 distinct lipid species were identified and quantified (Supplementary Table S1). Comparing the lipid species, ~210 statistically-significant differences ($p<0.05$) were revealed. In order to identify appropriate differences of relevance, data were analyzed and grouped for changes in

lipid class, fatty acyl chain length and degree of unsaturation. Based on such groupings, three major trends were revealed.

First, the average fatty acyl chain length decreased significantly in all sizeable membrane lipid classes when mature vs immature B cells were compared (Figure 3A). This difference reflects a more fluid membrane in mature A20 cells. Looking at the lipid species level, there was an increase in the most abundant shorter chain SM species with 16:0 fatty acyl chain (Supplementary Table S1; SM (34:1:2)).

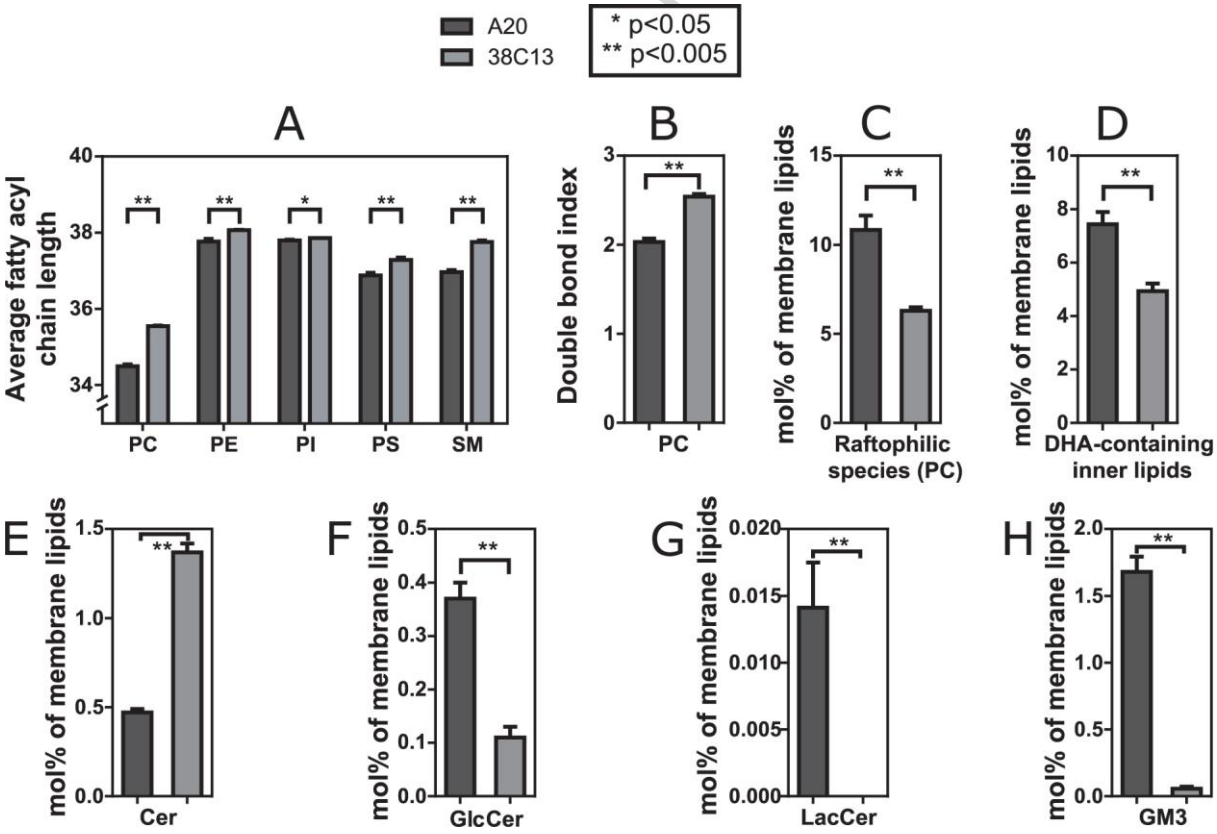

Figure 3. Lipidomic analysis revealed remarkable differences in membrane lipid composition of NT-forming mature (NT+, A20) and non-forming immature (NT-, 38C13) B cells. Alterations in the average chain length of individual membrane lipid classes PC, phosphatidylcholine; PE, phosphatidylethanolamine; PI, phosphatidylinositol; PS, phosphatidylserine; and SM, sphingomyelin (**A**). Difference in the double bond index of predominantly outer leaflet-resident PC (**B**). Difference in the level of raftophilic

phospholipid species (**C**). Difference in the contribution of docosahexaenoic acid (DHA)-containing and predominantly inner leaflet-resident phospholipid species (PE, PI and PS) to total membrane lipid composition (**D**). Alterations in the sphingolipid profile; Cer, ceramide; GlcCer, glucosyl ceramide; LacCer, lactosyl ceramide; GM3, monosialodihexosylganglioside (**E-H**). Values are expressed as mean ± SEM, n = 6-8; * $p<0.05$, ** $p<0.005$. 2-column width

Second, the double bond index, defined as the total moles of double bonds, was calculated. It represents acyl chain unsaturation level and showed a significantly lower level of dominantly outer leaflet-resident phosphatidylcholine (PC) in mature B cells (Figure 3B) compared to results for immature B cells. The decrease was a result of the increase in more highly saturated species (double bond number (db)=0-2) and concomitant lowering of more highly unsaturated species (db=3-7) Supplementary Table S1). This combined effect may undoubtedly enhance the ability of PC to induce positive curvature in the mature B cell membranes. In addition, we found that the membrane level of raft-forming [21,34] disaturated (db=0) PC species almost doubled (Figure 3C). Furthermore, docosahexaenoic acid (DHA)-containing phosphatidylethanolamine (PE), phosphatidylinositol (PI) and phosphatidylserine (PS) species were found at significantly elevated amounts in A20 relative to 38C13 cells (Figure 3D).

Third, we observed the most striking differences in the sphingolipid profiles for mature versus immature cells. The relative amount of ceramide (Cer), a unique lipid key to sphingolipid biosynthesis, was substantially lowered in mature A20 cell membranes (Figure 3E), whereas its upstream metabolic derivatives glucosyl ceramide (GlcCer), lactosyl ceramide (LacCer), and ganglioside GM3 were found at highly increased levels in mature A20 cell membranes compared to immature B cells (Figure 3F-H).

3.2. Targeted depletion/deprivation of raftophilic lipids suppresses NT formation between B cells

Since lipid rafts were previously implicated in coupling the PM to the cortical actin cytoskeleton [35], and F-actin is considered as a dynamic scaffolding element of NTs in lymphocytes [8,9,19], we tested how targeted modification of cell membrane levels of GSLs and cholesterol influence NT outgrowth in B cells. Depletion of membrane cholesterol by methyl-β-cyclodextrin (MBCD, Figure 4A) or inhibition of the limiting enzyme of cholesterol biosynthesis, HMG-CoA-reductase with simvastatin (Figure 4B) both significantly suppressed NT growth in A20 cells in a concentration-dependent manner.

SM and other sphingolipids are usually considered as basic building blocks of lipid rafts. Therefore, we next investigated how modification of their membrane levels influences NT formation. Fumonisin B1 inhibits the key enzyme of sphingolipid biosynthesis, ceramide synthase [36]. Thus, the inhibition is expected to decrease the total membrane sphingolipid level and, consequently, the number of lipid rafts. Pretreatment of A20 B cells with Fumonisin B1 prior to the 1 h culture for NT formation suppressed NT growth frequency in a concentration-dependent manner (Figure 4C). Data obtained with a phenotypically different, HeLa human cervical carcinoma cell line, further confirm this finding. Control HeLa mCAT8 cells grew typically multiple ($n \geq 2$) interconnecting NTs towards the adjacent cells (Figure 4E) under conditons aaplied for B cells. The CERT-deficient HeLa cells grew less than half NTs compared to the parental mCAT8 HeLa cells (Figure 4D and F).

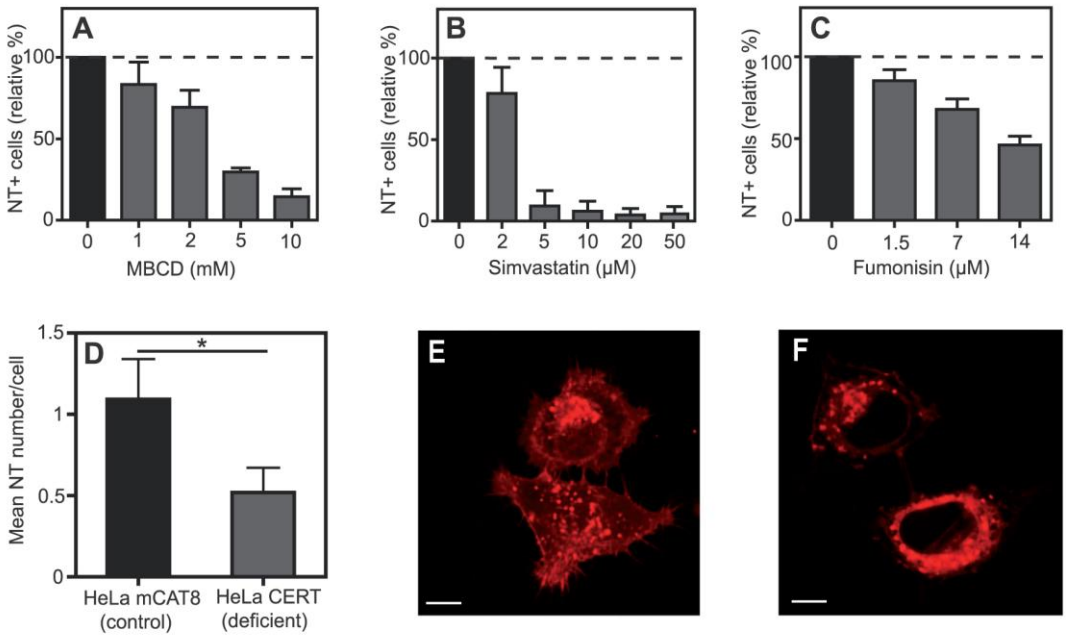

Figure 4. **Decreasing membrane levels of raftophilic lipids suppress NT formation in B cells**. Depletion of membrane cholesterol with MBCD, prior to 1 h culturing on fibronectin matrix for NT formation, significantly decreased the number of NT-forming (NT+) A20 cells in a concentration-dependent manner (**A**). Pretreatment of A20 cells with simvastatin, an inhibitor of cholesterol biosynthesis (**B**), or inhibition of ceramide synthase by Fumonisin B1 (**C**), also suppressed NT formation in a concentration-dependent manner. HeLa cells grew multiple connecting NTs at the conditions applied for B cells, as shown by the representative LC-CLSM image (**E**) (bar: 10μm). HeLa cells expressing mutant (dysfunctional) ceramide transporter (CERT) grew far fewer NTs than the parent control cell line (**D, F**). Note that the NT frequency in HeLa cells was defined as the average number of NTs/cell (**D**). The data for panels A-D represent at least 800 cells/sample and are displayed as mean ± SEM of three independent experiments. Cells were stained with DiI indocarbocyanine dye. 2-column width

These data, together with the Fumonisin B1 inhibition results in lymphocytes (Figure 4C), highlight that SM and sphingolipids, in general, are all essential PM components strongly promoting NT growth.

3.3. Membrane lipid composition and order are important determinants not only in formation, but also in mechanical properties of B cell nanotubes

Membrane tension and its mechanical feedback with membrane dynamics was earlier reported as an important regulator of cellular functions [37]. Therefore mechanical properties and lipid order of B cell NTs and PMs in context to the modulatory effects of targeted lipid modifications were also investigated. We demonstrated that NTs interconnecting B cells display a high degree of elasticity, shown by their surprisingly high resistance to repeated high-amplitude stretches exerted by an AFM cantilever tip (Supplementary Movie S1). NTs rapidly restored their original, contracted shape after stretching. Interestingly, a high amplitude oscillation of the NT, evoked by an adjacent resonating AFM cantilever, was also observed, indicating that NTs may behave as elastic chords under environmental tension levels (Supplementary Movie S2). These observations suggest that B cell NTs are sensitive to the coupled mechanics of their environment and do not adhere tightly to the extracellular matrix (ECM).

Next, we investigated how the elasticity of membrane NTs is affected by modification of membrane lipid levels and order. This was probed by detecting changes in dynamic membrane tension using „multiple tether" AFM technology described earlier [38]. As shown in Figure 5A, after pulling out multiple tethers from B cell surfaces using the cantilever tip by exceeding a certain tip-surface distance, the NTs are gradually ruptured or released as indicated by the sequential steps seen on the retraction curve (Figure 5B and C). Force

plateaus show that constant force is required to elongate the tethers. At each release or rupture event this force decreases to that needed to maintain a single (or occasionally multiple) tether(s) (Figure 5C), which was shown to be a predictive parameter of biophysical properties of the PM [39]. Rupture/release forces showed monomodal distributions (Supplementary Figure S1), and appeared to be fairly sensitive to the altered lipid composition/order of B cell membrane. Decreased membrane levels of sphingolipids, cholesterol or membrane fluidization (by short-term DHA treatment) all resulted in significantly smaller forces, while crosslinking of lipid rafts with anti-CTXB (ganglioside-XL) slightly increased the force (Figure 5D).

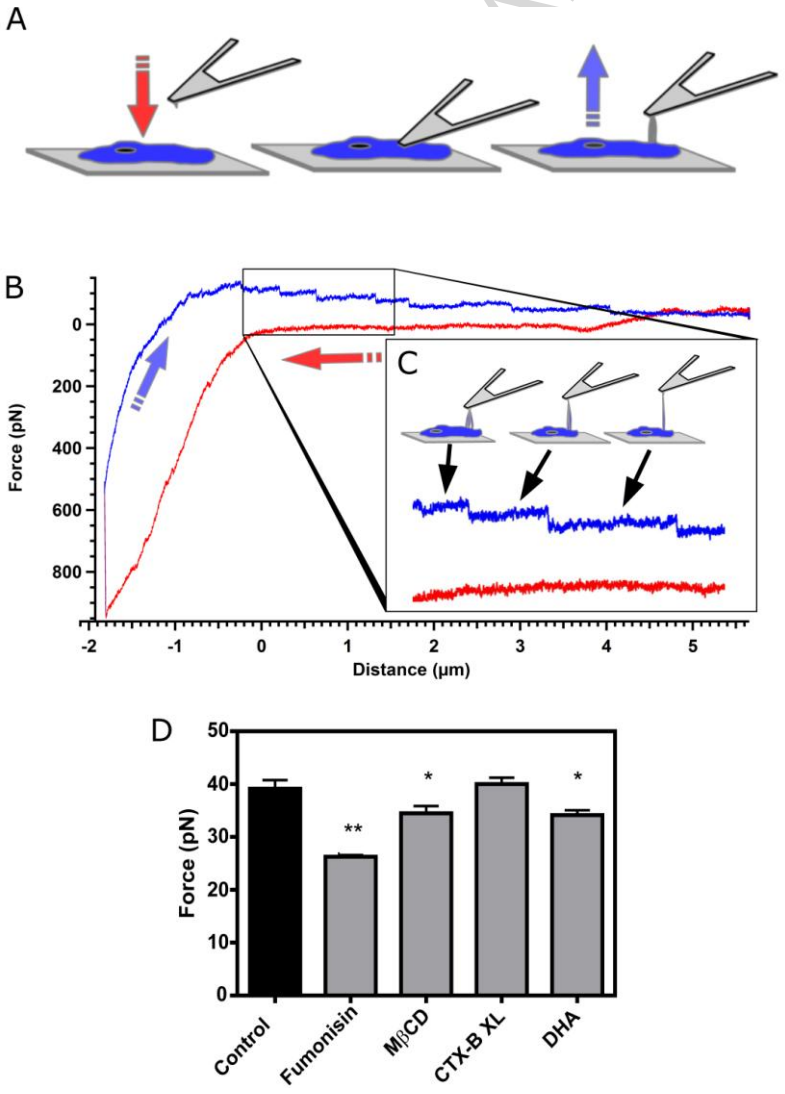

Figure 5. Plasticity of membrane tethers formed by AFM mechanomanipulation is sensitive to membrane lipid modifications. (**A**) Scheme of the micromanipulation measurement. The cantilever tip was advanced to the cell surface until contact. Then multiple NTs were pulled from the cells by gradually increasing the tip-cell surface distance. (**B**) Representative force graph of micromanipulation procedure depicted in (**A**). Red line, indicated by red arrow, shows how the cantilever approaches the cell surface. Zero distance corresponds to the point where the tip probed the cell surface. Following the interactions, the cantilever retracts, pulling several NTs (force curve: blue line; direction blue arrow). The enlarged panel **C** shows the force steps (pointed out by black arrows), indicating the gradual rupture/release of membrane tethers. The average magnitudes of force steps characteristic of control (untreated) or various membrane-modified A20 B cells are also shown (**D**). Cells were treated with 7 μM Fumonisin B to decrease membrane sphingolipid level, with 5 mM MBCD to decrease cholesterol level, with CTX-B plus anti-CTXB antibody to crosslink gangliosides, and with 20 μM DHA to fluidize the cell membrane. Data are expressed as mean ±SEM from at least three independent experiments (more than 150 force plateaus were evaluated for each sample); * $p \leq 0.05$; ** $p \leq 0.01$. 1,5-column width

These data suggest that the dynamic lipid composition of the PM can sensitively influence the elasticity and fluidity properties of the membrane, which, consequently, may influence NT growth.

Finally, we show how changes in the lipid bilayer order in B cell PMs relate to their NT-forming capacity. Lipid ordering was probed by using the di-4-ANEPPHQ polarimetric fluorescent probe [21,40]. Analyzing the generalized polarization (GP) derived from fluorescence images of NT membranes (Region of Interest (ROI) 1) and cell body membranes (ROI 2) of B cells, detected in two spectral channels (Figure 6A and B), revealed that the 'lipid packing density' of NTs (Figure 6C) is lower than that of PM of the cell body (Figure

6D). Short-term linoleic acid (LA, 200 μM) or DHA-treatment (fluidization) of B cells brought the PM lipid order into the range of NTs (Figure 6E) and also promoted NT formation (Figure 6F and G), while ganglioside crosslinking, increasing the lipid order, reduced NT frequency (Figure 6H).

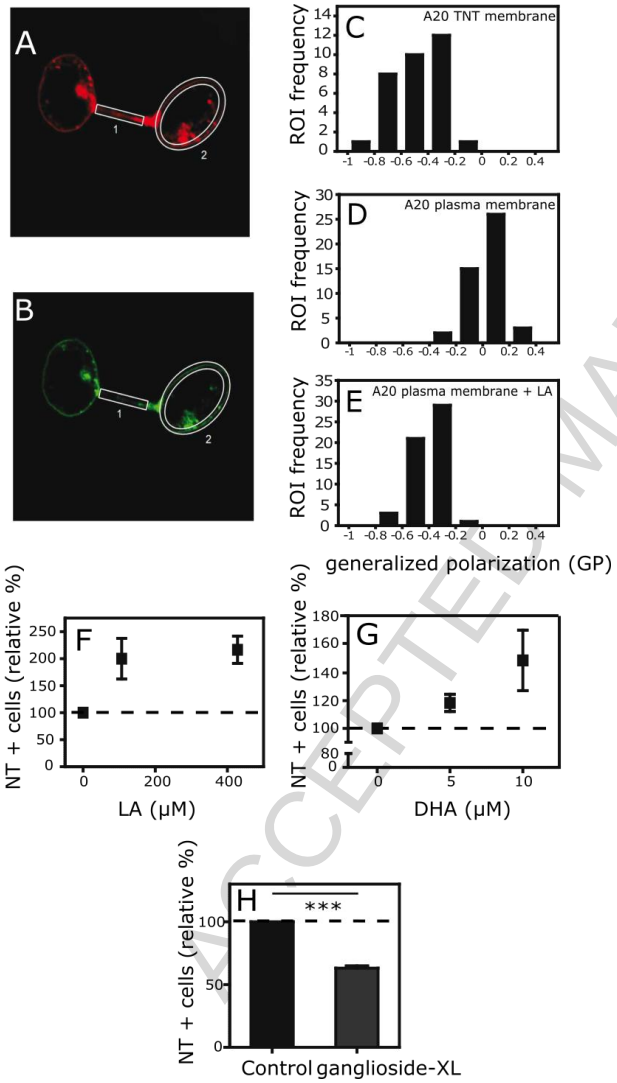

Figure 6. Relationship between membrane lipid order and NT growing capacity of B cells. The generalized polarization (GP) values in di-4-ANEPPDHQ-stained A20 cells were determined from images recorded in two emission channels $\Delta\lambda_1$: 505-560 nm (**A**) and $\Delta\lambda_2$: > 610 nm (**B**). Representative images of NT and cell body ROIs 1 and 2, respectively, are shown in panels **A** and **B**. GP values shown for panels C-E were determined from at least 80

ROIs in selected cellular regions. Fluidization of the cell membrane with LA (**F**) or DHA (**G**) remarkably increased NT formation. In contrast, increasing lipid ordering by crosslinking gangliosides using CTXB and anti-CTXB antibody (**H**) supressed NT formation. Data on panels **C-H** represent at least 800 cells/sample and are each displayed as mean ±SEM for three independent experiments. (1 column width).

These data, together with the results of the dynamic membrane tension tests (Figure 5) concordantly show that small changes in the membrane lipid composition can cause measurable changes in the molecular order and elasticity properties of the cell membrane that affect NT growth and mechanical stability.

4. Discussion

Membrane NTs are long-distance intercellular communication pathways mediating „on-tube" or „in-tube" transport of various objects. The goal of this study was to investigate the roles of composition, spatial organization and molecular order of lipids in cell membranes in formation of NTs between lymphocytes, primarily in B cells. Our results clearly demonstrate that maturation or differentiation through the dynamically changing lipid composition may regulate NT growth by various mechanisms.

First, the actual balance of cone and inverted cone-shaped lipids is recognized as a control of filopodia/NT growth. Lipidomic analysis revealed several remarkable differences between mature (spontaneously form NTs) and immature (not capable to form NTs) B cells. Mature B cells predominantly express outer leaflet-specific, inverted cone-shaped lipids, such as GSLs. In addition, the overall decrease in the unsaturation level of PC also enhances its positive curvature-forming propensity in the exoplasmic leaflet. Simultaneous enrichment of PUFA-containing phospholipid species (PE, PI and PS) can induce negative curvature in the

inner leaflet [41]. The only exception from the strong linear correlation of NT-frequency and ganglioside level was the 1-305 pre-B cell. In these cells the number of functional rafts (because of extremely low cholesterol level) is likely low, which may partly explain this behavior.

A special role can also be assigned to cholesterol in controlling NT growth, as shown by results in Figures 4 and 5. One of these roles has already been shown by Lokar *et al.* in tumor cells [42], where local density of cholesterol in the PM of tumor cells altered the local geometry (curvature) of the membrane bilayer and depletion of membrane cholesterol by MBCD significantly reduced the average positive membrane curvature. Here, membrane cholesterol level showed a nearly Gaussian relationship with respect to NT growth frequency. This suggests that an optimal cholesterol level is a prerequisite for NT growth in B cells, while too high levels may prevent NT growth, presumably via reducing membrane elasticity and fluidity. It is noteworthy that out of the three human Burkitt B lymphomas, only the Daudi could grow NTs, underlying the importance of ganglioside/cholesterol balance in NT formation. These observations suggest that the leaflet-specific increase of cone- and inverted cone-shaped lipids together with optimal cholesterol level may directly promote NT growth [43,44] in mature versus immature B cells.

Second, lipid rafts have already been proposed as membrane domains in B lymphocytes involved in many crucial immune functions, such as antigen presentation to T cells, or formation of stable immunological synapses [45,46][47]. Membrane cholesterol is involved in stabilization of these domains [15,39,48,49]. The special (and quantitative) role of cholesterol in determining architecture and domain organization of lymphocyte PM was demonstrated by the observation that moderate (nonlethal) cholesterol depletion by MBCD [50] causes dramatic functional changes in T cell signaling by aggregation of lipid rafts, increased tyrosine phosphorylation, ERK activation, and a moderate elevation of cytoplasmic

Ca^{2+} [51]. On the other hand, strong reduction of cholesterol level (depletion with ≥10 mM MBCD or treatment with atorvastatin, a HMG-CoA reductase inhibitor) resulted in inhibition of lymphocyte activation [52] and a decreased stability of the membrane-linked actin cytoskeleton [15]. Thus, lipid rafts can control NT growth in a different way, as well. In lymphoid cells, the PM rafts usually contain raft-associated adaptor membrane proteins, such as PAG or EBP50 ezrin-binding protein, that may mediate dynamic connections of the PM to the actin filament network [53,54]. Binding of pleckstrin homology domain proteins is also under control of cholesterol level and thus responsible for the dynamic coupling to the actin cytoskeleton [15]. In lymphocytes, among others, Ezrin was shown as one of the PI(4,5)P2-activated adaptors coupling F-actin to the PM domains [55].

Here we showed that NT-forming capacity of both murine and human B cells linearly correlate with their CTX-B binding capacity. Our lipidomic data has shown that, in contrast to human B cells with dominant GM1 expression, in mouse B cells GM3 is the dominant ganglioside, which can also bind to CTX-B [56]. These data taken together suggest that the instantaneous amount of cholesterol- and/or PI(4,5)P2-enriched microdomains in the PM may determine NT growth, since the lack of raft-cytoskeleton interaction/coupling would prevent it. Our data concerning the selective ganglioside and SM expression levels in B cells, and also the AFM data showing decreased keeping force in cholesterol- or SM-depleted cells, are in accordance with this hypothesis. Fumonisin inhibition experiments and the observations with CERT-deficient HeLa cells [25,57] (Figure 4 and 5) concordantly show the critical role of sphingolipid levels, in NT formation. The present data, together with our recent findings [19], show that the lipid rafts of lymphocytes may coordinate their NT growth through such coupling (see Figure 7).

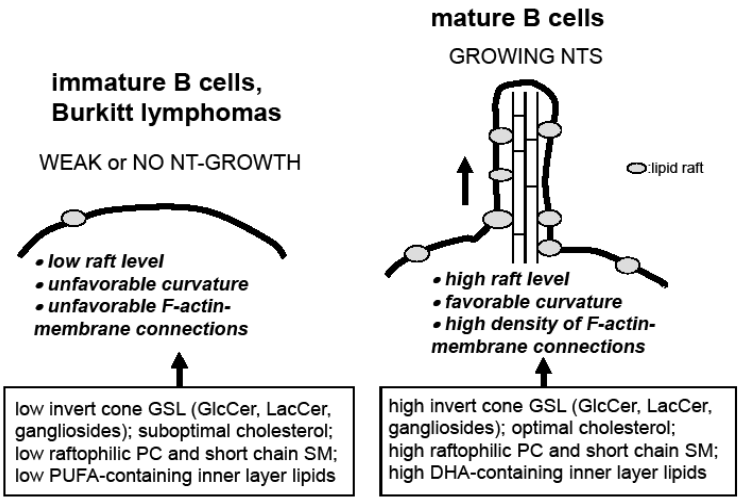

Figure 7. Schematic model of NT growth control by differentiation-dependent membrane lipid composition in lymphocytes. Lipid composition (and the consequent molecular order) of the plasma membrane may have a strong impact on the capability of B lymphocytes to grow nanotubular networks between each other. The model summarizes the three major points where the lipid composition may interefere with NT growth. These are: the balance of lipids with cone and inverted cone molecular geometry may promote favorably membrane curvature; balance of highly unsaturated lipids and cholesterol controls the membrane bending stiffness/plasticity; and the actual amount of lipid raft microdomains provides the linkage, among others, with the F-actin network.

The observed strikingly high mechanical stability and elasticity of B cell NTs assessed by AFM stretching tests (Supplementary Movie S1) suggest that the instantaneous bending stiffness and lipid ordering of the PM may be important physical determinants in NT growth frequency and stability. These findings also show that the membrane lipid reservoir buffering the dynamic membrane tension [58] probed in these experiments is considerable in B cells. The elasticity of B cell membrane was found sensitive to changes in lipid composition. Such

membrane modifications have been shown recently to affect microscopic anisotropy properties of the diIC18(3) lipid probe in human B cell membranes detected by Fluorescence Detected Linear Dichroism (FDLD) data from Differential-Polarization Confocal Laser Scanning microscopic measurements [59,60]. Consistent with this, imaging the lipid packing density-sensitive di-4-ANEPPDHQ probe [21] (Figure 6) further supported that, in B cells, the lipid order is an important determinant of membrane plasticity and also affects the frequency of NT growth. Membrane lipid order, determined by di-4-ANEPPDHQ fluorescent probe, showed diverse levels in helper T lymphocyte subpopulations in correlation with their function [61]. These data altogether suggest that cell differentiation- and/or function-dependent changes in membrane lipid composition/order of B lymphocytes may control not only their signalling but also their intercellular communication via NT connections.

Besides the dynamic lipid-determinants discussed above, several I-Bar (inverse BAR domain) proteins specifically binding to the PM may also play important, although indirect role in deforming the PM lipid bilayer, promoting curvature and thus resulting in growth of protrusions such as filopodia [62–65]. The N-terminal domain of IRSp53 (Insulin Receptor Substrate protein 53), expressed in B cells, was shown to bind negatively charged lipids, causing bending of the membrane and PI(4,5)P2 clustering [65,66]. Thus, its regulatory role in NT growth of B cells cannot be excluded and certainly warrants further detailed study.

Recently we have shown [19] that integrin receptor-ECM protein interactions, preferentially present in mature B lymphocytes, are essential in initiating NT growth. Since function, signaling and clustering of integrins also depend on their lipid microenvironment in the PM, it is conceivable to assume that a *functional assembly of lipid rafts and integrins* is an essential unit for formation of NTs. Particularly, raftophilic lipids may support NT formation in B cells either by promoting membrane curvature or by facilitating a coupling between these cholesterol-rich membrane domains and actin filaments. These results highlight the essential

role of lipid factors in controlling the outgrowth or retraction of NT structures between lymphocytes that may form new communication and transport pathways between two B cells or between B and T cells. In addition, such immunomodulatory pathways can also be considered as possible targets of therapeutic intervention using nanoparticle-bound drugs.

Acknowledgements

This work was supported by Hungarian National Science Fund (OTKA) by grants (T104971 to JM; NN 107776 and K112794 to MN; K109480 to MK; ANN 112372 and NN 111006 to LV, GB, MP) and sponsored in part, by MedinProt Project (Hungarian Academy of Sciences) to JM. We thank the National Development Agency (NFU) and the European Social Fund for supporting this project, in part, under Grant Agreement TÁMOP 4.2.1./B-09/1/KMR-2010-0003, and the Ministry for Hungarian National Economy for financing this work by GINOP-2.3.2-15-2016-00001; GINOP-2.3.2-15-2016-00006; GINOP-2.2.1-15-2016-00007 and GINOP -2.3.2-15-2016-00040.

The authors thank Dr. Péter Németh (Environmental Chemistry Research Group, Research Centre for Natural Sciences, Budapest, Hungary) for providing scanning electron microscopic images and to Drs. Mihály Kovács, Glória László, Andrea Balogh and Ibolya Horváth for valuable advice and discussions throughout the project, as well as to Ms. Márta Pásztor and Mr. Árpád Mikesy for their skillful technical assistance.

References

[1] G.M. Delgoffe, P.J. Murray, D.A. Vignali, Interpreting mixed signals: the cell's cytokine conundrum, Curr. Opin. Immunol., 23 (2011) 632–638.

[2] C. Théry, M. Ostrowski, E. Segura, Membrane vesicles as conveyors of immune responses, Nat. Rev. Immunol., 9 (2009) 581–593.

[3] B. György, T.G. Szabó, M. Pásztói, Z. Pál, P. Misják, B. Aradi, V. László, É. Pállinger, E. Pap, Á. Kittel, G. Nagy, A. Falus, E.I. Buzás, Membrane vesicles, current state-of-the-art: emerging role of extracellular vesicles, Cell. Mol. Life Sci., 68 (2011) 2667–2688.

[4] M.F. Krummel, M.D. Cahalan, The Immunological Synapse: a Dynamic Platform for Local Signaling, J. Clin. Immunol., 30 (2010) 364–372.

[5] M.L. Dustin, D. Depoil, New insights into the T cell synapse from single molecule techniques, Nat. Rev. Immunol., 11 (2011) 672–684.

[6] A. Rustom, R. Saffrich, I. Markovic, P. Walther, H.-H. Gerdes, Nanotubular highways for intercellular organelle transport, Science, 303 (2004) 1007–1010.

[7] B. Onfelt, S. Nedvetzki, K. Yanagi, D.M. Davis, Cutting edge: Membrane nanotubes connect immune cells, J. Immunol. Baltim. Md 1950, 173 (2004) 1511–1513.

[8] D.M. Davis, S. Sowinski, Membrane nanotubes: dynamic long-distance connections between animal cells, Nat. Rev. Mol. Cell Biol., 9 (2008) 431–436.

[9] H.-H. Gerdes, R.N. Carvalho, Intercellular transfer mediated by tunneling nanotubes, Curr. Opin. Cell Biol., 20 (2008) 470–475.

[10] B. Onfelt, S. Nedvetzki, R.K. Benninger, M.A. Purbhoo, S. Sowinski, A.N. Hume, M.C. Seabra, M.A. Neil, P.M. French, D.M. Davis, Structurally distinct membrane nanotubes between human macrophages support long-distance vesicular traffic or surfing of bacteria, J Immunol, 177 (2006) 8476–83.

[11] S.C. Watkins, R.D. Salter, Functional connectivity between immune cells mediated by tunneling nanotubules, Immunity, 23 (2005) 309–18.

[12] S. Sowinski, C. Jolly, O. Berninghausen, M.A. Purbhoo, A. Chauveau, K. Kohler, S. Oddos, P. Eissmann, F.M. Brodsky, C. Hopkins, B. Onfelt, Q. Sattentau, D.M. Davis, Membrane nanotubes physically connect T cells over long distances presenting a novel route for HIV-1 transmission, Nat Cell Biol, 10 (2008) 211–9.

[13] S. Abounit, C. Zurzolo, Wiring through tunneling nanotubes--from electrical signals to organelle transfer, J Cell Sci, 125 (2012) 1089–98.

[14] D.M. Davis, S. Sowinski, Membrane nanotubes: dynamic long-distance connections between animal cells, Nat. Rev. Mol. Cell Biol., 9 (2008) 431–436.

[15] J. Kwik, S. Boyle, D. Fooksman, L. Margolis, M.P. Sheetz, M. Edidin, Membrane cholesterol, lateral mobility, and the phosphatidylinositol 4,5-bisphosphate-dependent organization of cell actin, Proc Natl Acad Sci U A, 100 (2003) 13964–9.

[16] J. Storch, S.L. Shulman, A.M. Kleinfeld, Plasma membrane lipid order and composition during adipocyte differentiation of 3T3F442A cells Studies in intact cells with 1-[4-(trimethylamino)phenyl]-6-phenylhexatriene, J Biol Chem, 264 (1989) 10527–33.

[17] M. He, S. Guo, Z. Li, In situ characterizing membrane lipid phenotype of breast cancer cells using mass spectrometry profiling, Sci Rep, 5 (2015) 11298.

[18] L. Tuosto, I. Parolini, S. Schroder, M. Sargiacomo, A. Lanzavecchia, A. Viola, Organization of plasma membrane functional rafts upon T cell activation, Eur J Immunol, 31 (2001) 345–9.

[19] A. Osteikoetxea-Molnár, E. Szabó-Meleg, E.A. Tóth, Á. Oszvald, E. Izsépi, M. Kremlitzka, B. Biri, L. Nyitray, T. Bozó, P. Németh, M. Kellermayer, M. Nyitrai, J. Matko, The growth determinants and transport properties of tunneling nanotube networks between B lymphocytes, Cell. Mol. Life Sci., 73 (2016) 4531–4545.

[20] T. Parasassi, E. Gratton, W.M. Yu, P. Wilson, M. Levi, Two-photon fluorescence microscopy of laurdan generalized polarization domains in model and natural membranes, Biophys J, 72 (1997) 2413–29.

[21] D.M. Owen, C. Rentero, A. Magenau, A. Abu-Siniyeh, K. Gaus, Quantitative imaging of membrane lipid order in cells and organisms, Nat Protoc, 7 (2012) 24–35.

[22] Y. Caspi, M. Taya, N. Hollander, J. Haimovich, Light Chain Loss and Reexpression Leads to Idiotype Switch Surrogate Light Chains are Probably Responsible for this Process, in: M. Potter, F. Melchers (Eds.), Mech. B-Cell Neoplasia 1994, Springer Berlin Heidelberg, Berlin, Heidelberg, 1995: pp. 179–186.

[23] N. Haran-Ghera, A. Peled, L. Wu, K. Shortman, B. Brightman, H. Fan, The effects of passive antiviral immunotherapy in AKR mice: I The susceptibility of AKR mice to spontaneous and induced T cell lymphomagenesis, Leukemia, 9 (1995) 1199–206.

[24] H. Spits, J.E. De Vries, C. Terhorst, The cell-mediated lympholysis-inducing capacity of highly purified human monocytes and T lymphocytes in primary and secondary mixed leukocyte cultures, J. Immunol., 126 (1981) 2275–2278.

[25] T. Yamaji, K. Hanada, Establishment of HeLa cell mutants deficient in sphingolipid-related genes using TALENs, PLoS One, 9 (2014) e88124.

[26] O. Antal, M. Péter, L. Hackler Jr., I. Mán, G. Szebeni, F. Ayaydin, K. Hideghéty, L. Vigh, K. Kitajka, G. Balogh, L.G. Puskás, Lipidomic analysis reveals a radiosensitizing role of gamma-linolenic acid in glioma cells, Biochim. Biophys. Acta BBA - Mol. Cell Biol. Lipids, 1851 (2015) 1271–1282.

[27] E. Fahy, S. Subramaniam, R.C. Murphy, M. Nishijima, C.R. Raetz, T. Shimizu, F. Spener, G. van Meer, M.J. Wakelam, E.A. Dennis, Update of the LIPID MAPS comprehensive classification system for lipids, J Lipid Res, 50 Suppl (2009) S9-14.

[28] R. Herzog, D. Schwudke, K. Schuhmann, J.L. Sampaio, S.R. Bornstein, M. Schroeder, A. Shevchenko, A novel informatics concept for high-throughput shotgun lipidomics based on the molecular fragmentation query language, Genome Biol, 12 (2011) R8.

[29] J.D. Storey, R. Tibshirani, Statistical significance for genomewide studies, Proc. Natl. Acad. Sci., 100 (2003) 9440–9445.

[30] A. Biro, L. Cervenak, A. Balogh, A. Lorincz, K. Uray, A. Horvath, L. Romics, J. Matko, G. Fust, G. Laszlo, Novel anti-cholesterol monoclonal immunoglobulin G antibodies as probes and potential modulators of membrane raft-dependent immune functions, J Lipid Res, 48 (2007) 19–29.

[31] Z. Beck, A. Balogh, A. Kis, E. Izsepi, L. Cervenak, G. Laszlo, A. Biro, K. Liliom, G. Mocsar, G. Vamosi, G. Fust, J. Matko, New cholesterol-specific antibodies remodel HIV-1 target cells' surface and inhibit their in vitro virus production, J Lipid Res, 51 (2010) 286–96.

[32] M.S. Kellermayer, A. Karsai, A. Kengyel, A. Nagy, P. Bianco, T. Huber, A. Kulcsar, C. Niedetzky, R. Proksch, L. Grama, Spatially and temporally synchronized atomic force and total internal reflection fluorescence microscopy for imaging and manipulating cells and biomolecules, Biophys J, 91 (2006) 2665–77.

[33] J.L. Hutter, J. Bechhoefer, Calibration of atomic-force microscope tips, Rev. Sci. Instrum., 64 (1993) 1868–1873.

[34] S. Mukherjee, F.R. Maxfield, MEMBRANE DOMAINS, Annu. Rev. Cell Dev. Biol., 20 (2004) 839–866.

[35] B.P. Head, H.H. Patel, P.A. Insel, Interaction of membrane/lipid rafts with the cytoskeleton: impact on signaling and function: membrane/lipid rafts, mediators of cytoskeletal arrangement and cell signaling, Biochim Biophys Acta, 1838 (2014) 532–45.

[36] A.H. Merrill, M.C. Sullards, E. Wang, K.A. Voss, R.T. Riley, Sphingolipid metabolism: roles in signal transduction and disruption by fumonisins, Env. Health Perspect, 109 Suppl 2 (2001) 283–9.

[37] N.C. Gauthier, T.A. Masters, M.P. Sheetz, Mechanical feedback between membrane tension and dynamics, Trends Cell Biol., 22 (2012) 527–535.

[38] M. Sun, J.S. Graham, B. Hegedus, F. Marga, Y. Zhang, G. Forgacs, M. Grandbois, Multiple membrane tethers probed by atomic force microscopy, Biophys J, 89 (2005) 4320–9.

[39] M. Sun, N. Northup, F. Marga, T. Huber, F.J. Byfield, I. Levitan, G. Forgacs, The effect of cellular cholesterol on membrane-cytoskeleton adhesion, J Cell Sci, 120 (2007) 2223–31.

[40] L. Jin, A.C. Millard, J.P. Wuskell, H.A. Clark, L.M. Loew, Cholesterol-enriched lipid domains can be visualized by di-4-ANEPPDHQ with linear and nonlinear optics, Biophys J, 89 (2005) L04-6.

[41] W.E. Teague, O. Soubias, H. Petrache, N. Fuller, K.G. Hines, R.P. Rand, K. Gawrisch, Elastic Properties of Polyunsaturated Phosphatidylethanolamines Influence Rhodopsin Function, Faraday Discuss., 161 (2013) 383–459.

[42] M. Lokar, D. Kabaso, N. Resnik, K. Sepcic, V. Kralj-Iglic, P. Veranic, R. Zorec, A. Iglic, The role of cholesterol-sphingomyelin membrane nanodomains in the stability of intercellular membrane nanotubes, Int J Nanomedicine, 7 (2012) 1891–902.

[43] S. Jaikishan, J.P. Slotte, Effect of hydrophobic mismatch and interdigitation on sterol/sphingomyelin interaction in ternary bilayer membranes, Biochim. Biophys. Acta BBA - Biomembr., 1808 (2011) 1940–1945.

[44] V.L. Perillo, D.A. Peñalva, A.J. Vitale, F.J. Barrantes, S.S. Antollini, Transbilayer asymmetry and sphingomyelin composition modulate the preferential membrane

partitioning of the nicotinic acetylcholine receptor in Lo domains, Arch. Biochem. Biophys., 591 (2016) 76–86.

[45] H.A. Anderson, E.M. Hiltbold, P.A. Roche, Concentration of MHC class II molecules in lipid rafts facilitates antigen presentation, Nat Immunol, 1 (2000) 156–62.

[46] I. Gombos, C. Detre, G. Vamosi, J. Matko, Rafting MHC-II domains in the APC (presynaptic) plasma membrane and the thresholds for T-cell activation and immunological synapse formation, Immunol Lett, 92 (2004) 117–24.

[47] P. Friedl, J. Storim, Diversity in immune-cell interactions: states and functions of the immunological synapse, Trends Cell Biol, 14 (2004) 557–67.

[48] J. Matko, J. Szollosi, Landing of immune receptors and signal proteins on lipid rafts: a safe way to be spatio-temporally coordinated?, Immunol Lett, 82 (2002) 3–15.

[49] J. Matkó, J. Szöllősi, Regulatory Aspects of Membrane Microdomain (Raft) Dynamics in Live Cells, in: M.P. Mattson (Ed.), Membr. Microdomain Signal. Lipid Rafts Biol. Med., Humana Press, Totowa, NJ, 2005: pp. 15–46.

[50] M.P. Besenicar, A. Bavdek, A. Kladnik, P. Macek, G. Anderluh, Kinetics of cholesterol extraction from lipid membranes by methyl-beta-cyclodextrin--a surface plasmon resonance approach, Biochim Biophys Acta, 1778 (2008) 175–84.

[51] S. Mahammad, J. Dinic, J. Adler, I. Parmryd, Limited cholesterol depletion causes aggregation of plasma membrane lipid rafts inducing T cell activation, Biochim Biophys Acta, 1801 (2010) 625–34.

[52] N. Blank, M. Schiller, S. Krienke, F. Busse, B. Schatz, A.D. Ho, J.R. Kalden, H.M. Lorenz, Atorvastatin inhibits T cell activation through 3-hydroxy-3-methylglutaryl coenzyme A reductase without decreasing cholesterol synthesis, J Immunol, 179 (2007) 3613–21.

[53] N. Brdickova, T. Brdicka, L. Andera, J. Spicka, P. Angelisova, S.L. Milgram, V. Horejsi, Interaction between two adapter proteins, PAG and EBP50: a possible link between membrane rafts and actin cytoskeleton, FEBS Lett, 507 (2001) 133–6.

[54] K. Itoh, M. Sakakibara, S. Yamasaki, A. Takeuchi, H. Arase, M. Miyazaki, N. Nakajima, M. Okada, T. Saito, Cutting edge: negative regulation of immune synapse formation by anchoring lipid raft to cytoskeleton through Cbp-EBP50-ERM assembly, J Immunol, 168 (2002) 541–4.

[55] M. Fritzsche, C. Erlenkämper, G.T. Charras, K. Kruse, C. Eggeling, Homeostasis of the Cellular Actin Cortex, Biophys. J., 106 (2014) 735a.

[56] G.M. Kuziemko, M. Stroh, R.C. Stevens, Cholera Toxin Binding Affinity and Specificity for Gangliosides Determined by Surface Plasmon Resonance, Biochemistry (Mosc.), 35 (1996).

[57] K. Hanada, K. Kumagai, S. Yasuda, Y. Miura, M. Kawano, M. Fukasawa, M. Nishijima, Molecular machinery for non-vesicular trafficking of ceramide, Nature, 426 (2003) 803–9.

[58] D. Raucher, M.P. Sheetz, Characteristics of a membrane reservoir buffering membrane tension, Biophys. J., 77 (1999) 1992–2002.

[59] I. Gombos, G. Steinbach, I. Pomozi, A. Balogh, G. Vamosi, A. Gansen, G. Laszlo, G. Garab, J. Matko, Some new faces of membrane microdomains: a complex confocal fluorescence, differential polarization, and FCS imaging study on live immune cells, Cytom. A, 73 (2008) 220–9.

[60] G. Steinbach, K. Pawlak, E.A. Tóth, A. Molnár, J. Matkó, G. Garab, Mapping microscopic order in plant and mammalian cells and tissues: novel differential polarization attachment for new generation confocal microscopes (DP-LSM), Methods Appl. Fluoresc., 2 (2014) 015005.

[61] L. Miguel, D.M. Owen, C. Lim, C. Liebig, J. Evans, A.I. Magee, E.C. Jury, Primary human CD4+ T cells have diverse levels of membrane lipid order that correlate with their function, J Immunol, 186 (2011) 3505–16.

[62] H.T. McMahon, J.L. Gallop, Membrane curvature and mechanisms of dynamic cell membrane remodelling, Nature, 438 (2005) 590–6.

[63] S. Ahmed, W.I. Goh, W. Bu, I-BAR domains, IRSp53 and filopodium formation, Semin Cell Dev Biol, 21 (2010) 350–6.

[64] H. Zhao, A. Pykalainen, P. Lappalainen, I-BAR domain proteins: linking actin and plasma membrane dynamics, Curr Opin Cell Biol, 23 (2011) 14–21.

[65] J. Saarikangas, H. Zhao, A. Pykalainen, P. Laurinmaki, P.K. Mattila, P.K. Kinnunen, S.J. Butcher, P. Lappalainen, Molecular mechanisms of membrane deformation by I-BAR domain proteins, Curr Biol, 19 (2009) 95–107.

[66] K. Futo, E. Bodis, L.M. Machesky, M. Nyitrai, B. Visegrady, Membrane binding properties of IRSp53-missing in metastasis domain (IMD) protein, Biochim Biophys Acta, 1831 (2013) 1651–5.